

This is the author-created version of the following work:

O'Brien, Paul A., Tan, Shangjin, Yang, Chentao, Frade, Pedro R., Andreakis, Nikolaos, Smith, Hillary A., Miller, David J., Webster, Nicole S., Zhang, Guojie, and Bourne, David G. (2020) *Diverse coral reef invertebrates exhibit patterns of phyllosymbiosis*. ISME Journal: multidisciplinary journal of microbial ecology, 14 pp. 2211-2222.

Access to this file is available from:

<https://researchonline.jcu.edu.au/63428/>

© The Author(s), under exclusive licence to International Society for Microbial Ecology 2020

Please refer to the original source for the final version of this work:

<https://doi.org/10.1038/s41396%2D020%2D0671%2Dx>

1
2
3
4
5
6
7
8
9
10
11
12
13
14
15
16
17
18
19
20
21
22
23
24
25
26
27
28
29
30
31
32
33

Diverse coral reef invertebrates exhibit patterns of phylosymbiosis

Paul A. O'Brien^{1,2,3,4}, Shangjin Tan⁵, Chentao Yang⁵, Pedro R. Frade⁶, Nikos Andreakis¹ Hillary
A. Smith¹, David J. Miller^{2,7}, Nicole S. Webster^{3,4,8}, Guojie Zhang^{5,9,10,11}, David G. Bourne^{1,2,3,4}

¹ College of Science and Engineering, James Cook University, Townsville, QLD, Australia

² Centre for Tropical Bioinformatics and Molecular Biology, James Cook University, Townsville, QLD, Australia

³ Australian Institute of Marine Science, Townsville, QLD, Australia

⁴ AIMS@JCU, Townsville, QLD, Australia

⁵ BGI-Shenzhen, Beishan Industrial Zone, Shenzhen 518083, China

⁶ Centre of Marine Sciences, University of Algarve, Faro, Portugal

⁷ ARC Centre of Excellence for Coral Reef Studies, James Cook University, Townsville, QLD, Australia

⁸ Australian Centre for Ecogenomics, University of Queensland, Brisbane, QLD, Australia

⁹ Section for Ecology and Evolution, Department of Biology, University of Copenhagen, DK-2100 Copenhagen, Denmark

¹⁰ State Key Laboratory of Genetic Resources and Evolution, Kunming Institute of Zoology, Chinese Academy of Sciences, Kunming 650223, China

¹¹ Center for Excellence in Animal Evolution and Genetics, Chinese Academy of Sciences, Kunming 650223, China

Corresponding authors:

- Guojie Zhang zhanggj@genomics.cn
- David G. Bourne david.bourne@jcu.edu.au

34 Abstract

35 Microbiome assemblages of plants and animals often show a degree of correlation with host
36 phylogeny; an eco-evolutionary pattern known as phylosymbiosis. Using 16S rRNA gene
37 sequencing to profile the microbiome, paired with COI, 18S rRNA and ITS1 host phylogenies,
38 phylosymbiosis was investigated in four groups of coral reef invertebrates (scleractinian
39 corals, octocorals, sponges and ascidians). We tested three commonly used metrics to
40 evaluate the extent of phylosymbiosis: (a) intraspecific versus interspecific microbiome
41 variation, (b) topological comparisons between host phylogeny and hierarchical clustering
42 (dendrogram) of host-associated microbial communities, and (c) correlation of host
43 phylogenetic distance with microbial community dissimilarity. In all instances, intraspecific
44 variation in microbiome composition was significantly lower than interspecific variation.
45 Similarly, topological congruency between host phylogeny and the associated microbial
46 dendrogram was more significant than would be expected by chance across all groups,
47 except when using unweighted UniFrac distance (compared with weighted UniFrac and
48 Bray–Curtis dissimilarity). Interestingly, all but the ascidians showed a significant positive
49 correlation between host phylogenetic distance and associated microbial dissimilarity. Our
50 findings provide new perspectives on the diverse nature of marine phylosymbioses and the
51 complex roles of the microbiome in the evolution of marine invertebrates.

52

53 Introduction

54 Phylosymbiosis occurs when microbial community relationships reflect the evolutionary history of the
55 host [1–3]. The term was first coined to describe the impact of a host phylogenetic signal on gut microbial
56 community relationships in *Nasonia parasitoid* wasps [2, 4], and the phenomenon has since been
57 investigated in a diverse range of taxa and environments, e.g., the gut microbiomes of mammals and
58 insects [1, 5, 6], the skin microbiome of ungulates [7], the endolithic microbiome of coral [8] and the root
59 microbiome of plants [9]. These studies have confirmed that phylosymbiosis occurs in the simplest as
60 well as the most diverse microbial communities and the discovery of virus/host phylosymbioses [10]
61 demonstrates that the phenomenon is not limited to prokaryotes. As phylosymbiosis has become more
62 frequently observed, the mechanisms underpinning these patterns are of increasing interest.

63 Evolutionary processes such as codivergence and coevolution are distinct from phylosymbiosis,
64 establishing the need of an alternative term [1]. Namely, phylosymbiosis is a pattern observed at one
65 moment in time and space, which does not assume a stable evolutionary association between a host and
66 its microbiota or congruent ancestral splits, nor does it assume vertical transmission of microbial
67 symbionts [11]. While it is possible that different evolutionary processes contribute to the mechanisms
68 behind phylosymbiosis [8, 12], complex and dynamic systems that acquire high numbers of microbes
69 from the environment are likely structured by other mechanisms. For example, horizontal transmission of
70 microbes filtered through phylogenetically congruent host traits, biogeography of a host and the
71 microbiota, and dispersal of microbes among conspecifics all potentially contribute to observed
72 phylosymbiosis patterns [12–15]. These explanations are not necessarily mutually exclusive. Within a
73 complex microbiome where both vertical and horizontal transmission occurs among obligate and
74 facultative microbial members, phylosymbiosis is expected to rely on multiple mechanisms [3, 6].

75 Despite the extensive literature supporting phylo-symbiotic relationships, host phylogeny does not
76 always correlate with microbial community (dis)similarity. For example, in contrast to other mammals,
77 no significant congruence was observed between skin microbiome composition and host phylogeny in the
78 case of carnivores [7]. Similarly, no phylosymbiotic signal could be detected in the case of the intestinal
79 microbiota of 59 Neotropical birds [16] and the gut microbiomes of bats are more similar to birds than
80 other mammals [17]. There are multiple reasons why phylosymbiosis may not occur. First, factors such as

81 environment and diet may obscure phylosymbiotic signals, which have been successfully controlled for in
82 some studies [1, 4]. Second, in some cases, host genotype exerts strong effects on microbiome
83 composition that are independent of host phylogeny [8, 18, 19]. Finally, host physiology can structure the
84 microbiome [20], however, physiological traits may not always be consistent with host phylogeny [21].
85 Therefore, patterns of phylosymbiosis may be dependent on a certain host taxonomic level (i.e., host
86 family), where host genotype effects are reduced and host physiological traits and phylogeny are
87 congruent.

88 Reef invertebrates provide interesting opportunities for testing hypotheses of phylosymbiosis, as they
89 often host diverse microbial communities acquired by combinations of vertical and horizontal
90 transmission [22–25] that can be dynamic among different environments [26, 27]. Here, we first
91 characterise the microbiomes of four groups of coral reef invertebrates: scleractinian corals, octocorals,
92 sponges and ascidians. We then test three recommended analyses to investigate phylosymbiosis: (a)
93 comparison of intraspecific and interspecific variation in microbiome composition, (b) comparison of the
94 topology of host phylogeny and hierarchical clustering of its associated microbial community, and (c)
95 correlation of host phylogenetic distance with microbial community dissimilarity [3, 14]. We hypothesise
96 that a phylosymbiotic signal will be found across all four groups to show that host phylogeny is a
97 dominant factor in microbiome structure of reef invertebrates. Through an improved understanding of
98 microbial community dynamics using phylosymbiosis, our knowledge of how a microbiome is structured
99 and maintained in complex marine holobionts will be enhanced [25].

100 **Materials and methods**

101 **Sample collection**

102 Tissue samples from 3 to 5 replicates of 30 species of coral reef invertebrates (12 corals, 10 octocorals, 5
103 sponges and 3 ascidians) were collected on SCUBA from seven locations across the central and northern
104 sectors of the Great Barrier Reef (GBR) (Table S1; Fig. S1). On sampling trips to Broadhurst Reef, Davies
105 Reef and Orpheus Island, August 2017 (Table S1), adult colonies no larger than 30 × 30 cm were collected
106 using hammer and chisel and returned to the reef after sampling. Alternatively, sampling of invertebrates
107 was performed in situ. On the surface, colonies/samples were isolated and placed in running seawater
108 (0–2 h) until processing. Each invertebrate was sampled for 3–5 fragments ~5 cm in length using either a
109 hammer and chisel or dive knife (coral), or sterile razor blades (all other invertebrates). In addition,
110 seawater samples were collected from the central GBR sites in August 2017 as an environmental control
111 (Table S1). All samples were collected under the marine parks permits G12/35236.1 and G15/37574.1

112 **Sample processing and preservation**

113 Fragments were rinsed in autoclaved calcium- and magnesium-free seawater (CMFSW; NaCl: 26.2 g, KCl:
114 0.75 g, Na₂SO₄: 1 g, NaHCO₃: 0.042 g, per 1 L) to remove any loosely attached microbes. For scleractinian
115 coral, tissue was removed from the skeleton by pressurised air into ~30ml of CMFSW. Coral blastate was
116 homogenised by vortex for 1 min and 2 × 2 ml aliquots were kept for DNA extraction. Aliquots were
117 centrifuged for 10 min at 10,000 × g, the supernatant was removed, and tissue pellet was either snap
118 frozen in liquid nitrogen or preserved in 1 ml dimethyl sulfoxide-EDTA salt saturated solution (DESS) and
119 kept at –80 °C (Table S1). For octocorals and sponges, fragments were cut into small pieces ~0.5 × 0.5 cm³
120 using a sterile razor blade, snap frozen in a 2 ml cryovial and stored at –80 °C until DNA extraction.
121 Alternatively, a 15 ml falcon tube with ~7 ml DESS was filled with the dissected tissue until
122 approximately a 1:1 ratio of tissue:DESS was reached. The ascidians *Lissoclinum patella* and *Polycarpa*
123 *aurata* were dissected longitudinally and the tunic layer was removed and snap frozen as described
124 above. Colonies of the remaining ascidian *Didemnum molle* were dissected into three equal parts as the
125 tunic was too small to isolate and preserved in 1 ml DESS and kept at –80 °C. Seawater was collected from
126 each site (excluding the Ribbon Reefs (RR) and Osprey Reef) ~1 m above the benthos at the area of
127 sample collection using 4 × 5L retractable water bottles (washed and sterilised with 10% hydrochloric
128 acid). Approximately 2–3 L were then filtered through 0.22 µm sterivex filters and stored at –80 °C
129 (where –80 °C was not available, samples were stored at –20 °C for 1–5 days before being transferred to
130 –80 °C upon returning to the lab).

131 **DNA extraction and sequencing**

132 Approximately 0.05 g of tissue was used for DNA extraction using the DNeasy PowerBiofilm Kit (QIAGEN
133 Pty Ltd, VIC Australia 3148). Extraction was performed following the manufacturers protocol with the
134 BioSpec Mini- Beadbeater-96 used for mechanical lysis at 3–5 cycles of 30–60 s depending on the
135 difficulty to break down the tissue. Genomic DNA was sent to the Ramaciotti Centre for Genomics (UNSW,
136 Sydney Australia) for 16S rRNA amplicon sequencing on the Illumina MiSeq platform using the modified
137 V4 region primer set, 515F (GTGYCAGCM GCCGCGGTAA) [28] and 806R (GGACTACNVGGGT WTCAAT)
138 [29]. Samples were prepared for sequencing with the Earth Microbiome Project's 16S Illumina Amplicon
139 protocol and sequencing was performed following the standard Illumina protocol for 16S rRNA gene
140 amplicon library prep. Sequencing of the host phylogenetic markers COI, 18S rRNA and ITS1 was
141 performed at the Beijing Genome Institute following the BGISEQ-500 library prep protocol on the
142 BGISEQ-SE400 module. COI (~712 bp), 18 S (~470 bp) and ITS1 (~288 bp) were amplified using the
143 primer pairs, LCO1490 (GGTCAACAAATCATAAAGAT ATTGG) and HCO2198 (TAAACTTCAGGGTGACCA
144 AAAAATCA) for COI [30] and V4_18S_Next.For (CCAGCASCYCGGTAATTCC) and V4_18S_Next.Rev. B
145 (ACTBTCGYTCTTGATYARNGA) were modified from Pirredda et al. [31] for 18S rRNA. For ITS1, the
146 custom primers 18S-F1759 (GGTGAACCTGCGGAWGGATC) and 5.8S-R40 (CGCASYTDGCTGCGTTCTTC)
147 were designed by retrieving all available sequences from our target species and aligning them using
148 MAFFT [32]. Full length barcodes were assembled from single-end 400bp reads using the HIFI-SE
149 pipeline [33].

150 **16S rRNA gene amplicon analysis**

151 Sequences were analysed using QIIME2 (v 2018.4) [34] by first demultiplexing reads and denoising
152 following the DADA2 pipeline [35]. Taxonomic assignment was performed using a Naive Bayes classifier
153 pre-trained on the Silva 132 99% OTU database modified to the V4 region primer set 515F/806R. The
154 resulting amplicon sequence variant (ASV) table was filtered for chloroplast, mitochondrial and
155 eukaryotic sequences. A phylogenetic tree was reconstructed using the qiime fragment-insertion sepp
156 command (QIIME2 v 2019.1), which places the ASVs into a larger, well-curated 16S rRNA reference
157 phylogeny containing >200,000 representative tips (GreenGenes 13.8, 99% OTU) [36]. The resulting tree
158 was then trimmed to the original reference sequences and used for subsequent UniFrac analyses. ASV and
159 taxonomic tables were imported into R studio v.3.5.0 [37] for further analysis with extensive use of the
160 packages 'phyloseq' [38], 'vegan' [39], 'ggplot2' [40], 'ggtree' [41], 'ape' [42], 'phangorn' [43] and 'dplyr'
161 [44].

162 **Characterisation of microbial diversity and composition**

163 The following analyses were conducted at the ASV level, excluding visual representations of relative
164 abundance. Relative abundance for each microbial phylum was calculated and grouped by invertebrate
165 taxonomy to give a broad overview of microbial profiles of each invertebrate group. In addition, the top
166 25 most abundant microbial families across the entire dataset were shown to give an overview of the
167 lower taxonomic levels. As the taxonomic profile of the blanks was sufficiently different from the marine
168 invertebrate profiles, with only 0.4% of sequences present in the top 25 family level ASVs, these samples
169 were removed from further analysis. Rarefaction curves were calculated and plotted to illustrate the total
170 diversity of ASVs captured against the sampling effort. Alpha diversity was calculated using both species
171 richness (total number of ASVs retrieved per sample) and Shannon–Wiener diversity index on a dataset
172 rarefied to 3500 sequences (equal to the sample with the lowest number of sequences). Beta diversity
173 was calculated on non-rarefied data using the Bray–Curtis dissimilarity measure by first standardising
174 the data by the species maximum and then by the sample total (Wisconsin double standardisation). This
175 method of normalisation was chosen for beta diversity as transforming data to proportions returns the
176 most accurate Bray–Curtis dissimilarities [45]. The resulting dissimilarity scores were visualised using
177 non- metric multidimensional scaling (NMDS) to observe overall patterns in microbial community
178 structure among the different invertebrates. Analysis of variance (ANOVA) and a post-hoc Tukey's test
179 with unplanned comparisons and a Bonferroni correction were used for significance testing of alpha
180 diversity, while permutational multivariate analysis of variance (PERMANOVA) was used for beta
181 diversity using the pairwiseAdonis function for post-hoc analysis.

182 **Host phylogenetic reconstructions**

183 Representative sequences for COI, 18S rRNA and ITS1 from each species in each taxonomic group were
184 aligned separately using MUSCLE [46] and then concatenated using DAMBE [47]. Concatenated octocoral
185 and sponge alignments were further curated using Gblocks [48] to remove poorly aligned, high gap
186 regions. Evolutionary model selection was performed using JModelTest2 (Supplementary Table 2) [49]
187 and phylogenetic analysis was conducted in Mr Bayes v3.2.7 [50] using the outgroups *Carteriospongia*
188 *foliascens* for corals, octocorals and ascidians and *Cladiella* sp. for sponges. Outgroups were selected
189 based on their low phylogenetic relatedness to the ingroup and low variability in microbiome
190 composition among sample replicates. Evolutionary history was inferred using Bayesian inference with
191 the Markov Chain Monte Carlo method using two independent runs of 5,000,000 generations and all
192 models converged at <0.01.

193 **Phylosymbiosis analysis**

194 The 16S rRNA gene dataset was subsampled to each taxonomic group and analysed independently.
195 Gorgonians did not contain enough species within our dataset to compare host phylogeny with microbial
196 composition and were added to the soft coral dataset to create an octocoral group. Intraspecific against
197 interspecific variability of microbiome composition was compared using pairwise comparisons of Bray–
198 Curtis dissimilarity between each sample. Welch's t test was used for significance testing following an
199 arcsine transformation to normalise the 0–1 distribution, while an ANOVA and post-hoc Tukey's test with
200 unplanned comparisons and a Bonferroni correction were used to test for significant differences in
201 intraspecific variation among invertebrate groups.

202 Microbial dendrograms were built in QIIME2 using the qiime diversity beta-rarefaction command. Within
203 each invertebrate ASV table subset, all ASVs that appear two times or less and those that are present in
204 only one sample were removed to reduce noise from potentially spurious and transient ASVs. Each
205 sample was then pooled by host species and rarefied over 1000 iterations to the host species with the
206 lowest number of reads following the method of Brooks et al. [1]. Hierarchical clustering of host species
207 from the resulting table was performed using the UPGMA clustering method based on Bray–Curtis
208 dissimilarity and both weighted and unweighted UniFrac distances. Microbial dendrograms along with
209 phylogenetic trees and pooled ASV tables were imported into R studio for analysis.

210 To assess topological congruency, host phylogenetic tree topology was compared with the microbial
211 dendrograms using the normalised Robinson–Foulds (nRF) metric, where 0 is complete congruence and 1
212 is no congruence. Branch lengths were removed in host phylogenetic trees for visualisation and a
213 significance value was calculated using the RFmeasures function [14] with 9999 permutations.
214 Correlation between host phylogenetic distance and microbial dissimilarity was analysed by first creating
215 a distance matrix of pairwise phylogenetic distances between each host species and distance matrices of
216 Bray–Curtis dissimilarity and weighted and unweighted UniFrac distances using the pooled ASV tables. A
217 Mantel test was used to test for correlation between host and microbial distance matrices using Pearson
218 correlation with 9999 permutations. A similarity percentages (SIMPER) analysis was used to identify
219 which ASVs were contributing to dissimilarity between host species that showed incongruence.

220 **Results**

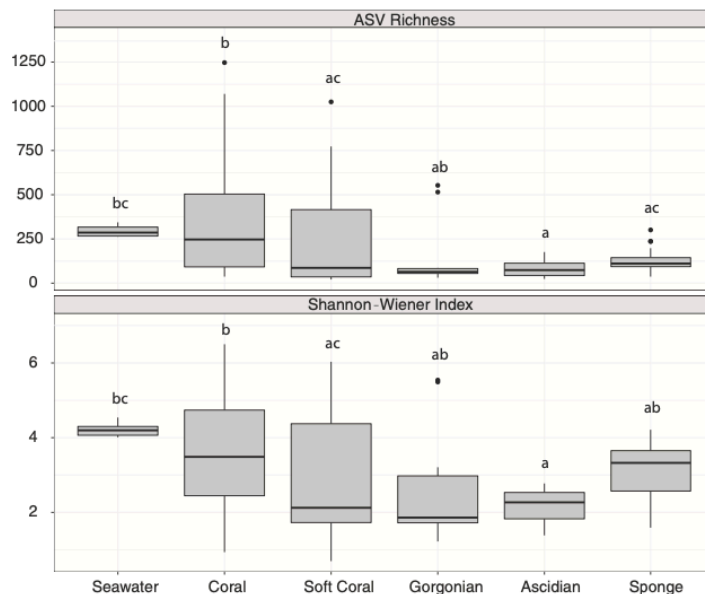
221 **Sample collection and sequencing**

222 Field collections resulted in a total of 161 samples across 30 species of reef invertebrates (Table S1). In
223 addition, eight seawater samples, two blank extractions and two sequencing positive controls were
224 sequenced. For 16S rRNA amplicon sequencing, this yielded a total of 10,415,183 reads in 173 samples,
225 which was reduced to 8,611,147 high quality reads following quality control and denoising. For host
226 phylogeny, successful COI sequences were obtained for all 30 species, however, 18S rRNA sequencing was
227 unsuccessful for *Acropora formosa*, *Acropora hyacinthus*, *Diploastrea heliopora*, *Heteroxenia* sp. and *Isis*
228 *hippuris* and ITS1 sequencing was unsuccessful for *Lissoclinum patella* and *Didemnum mole*. As a result,
229 ITS1 was not used for ascidian phylogeny.

230 Characterisation of microbial diversity and composition

231 Rarefaction curves for each sample approached asymptotes, illustrating that total ASV richness for each
232 sample was captured (Fig. S2). However, rarefaction to the sample with the lowest number of reads (*Isis*
233 *hippuris*: 3323 reads; excluding blanks) resulted in a loss in diversity in some samples. Nonetheless,
234 overall trends showed that both ASV richness and ASV diversity (Shannon–Wiener Index) were both
235 significantly different across the broad taxonomic associations (richness; ANOVA; $F_{(5, 163)} = 7.01$, $p <$
236 0.001 ; Fig. 1) (Shannon diversity; ANOVA; $F_{(5, 163)} = 4.64$, $p < 0.001$; Fig. 1). Post-hoc comparisons revealed
237 that seawater had a significantly higher ASV richness than the ascidians ($p = 0.024$), while coral had a
238 significantly higher ASV richness than ascidians ($p = 0.006$), soft corals ($p = 0.006$) and sponges ($p =$
239 0.003). For ASV diversity, post-hoc comparisons revealed an increase in diversity in coral compared with
240 the ascidians ($p = 0.009$) and soft corals ($p = 0.046$), and an increase in seawater compared with the
241 ascidians ($p = 0.014$). However, unlike richness, no difference was seen in ASV diversity between corals
242 and sponges ($p = 1.0$).

243



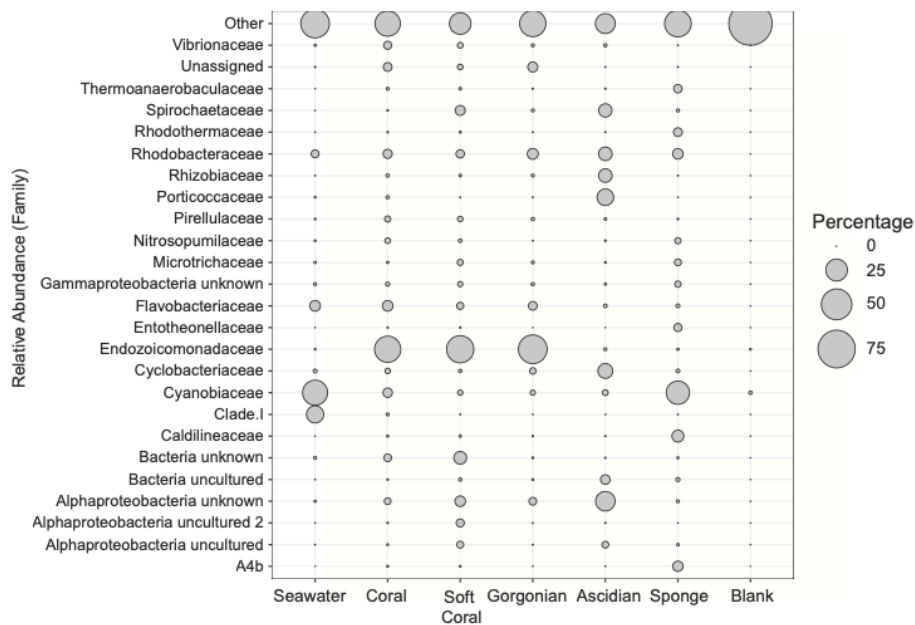
244

245 **Fig. 1** ASV richness (top panel) and Shannon–Wiener diversity index (bottom panel) for each invertebrate
246 group and seawater. Letters indicate groups which are significantly different from each other.

247 A total of 62 microbial phyla were observed across the invertebrate groups and microbial profiles showed
248 a high degree of uniformity at the phylum level. Microbial taxonomy mentioned here and herein are ASV
249 sequences affiliated to that taxonomic classification, with *Proteobacteria*, *Cyanobacteria* and *Bacteroidetes*
250 among the dominant phyla across all marine invertebrates (Fig. S3). However, differences were evident
251 even at the broad taxonomic level, with the octocorals (soft coral and gorgonians) hosting a higher
252 relative abundance of *Tenericutes* (mean = $4.71\% \pm 1.63$ SE and $11.12\% \pm 6.28$ SE, respectively)
253 compared with other invertebrates, while sponges were associated with more *Chloroflexi*, *Acidobacteria*
254 and *Cyanobacteria* (mean = $19.09\% \pm 2.29$ SE, $9.86\% \pm 1.64$ SE, and $28.31\% \pm 3.67$ SE, respectively).

255 Relative abundance at the family level indicated far more variation in taxonomic profiles among the
256 invertebrate groups (Fig. 2). The three groups of anthozoans (coral, soft coral and gorgonian) were
257 clearly different to the other marine invertebrate classifications and mostly dominated by the common
258 *Endozoicomonadaceae* (mean = $33.52\% \pm 4.19$ SE, $38.41\% \pm 4.58$ SE and $42.88\% \pm 10.74$ SE,
259 respectively). Sponges consisted of a high relative abundance of *Cyanobiaceae* (mean = $27.87\% \pm 3.74$ SE),
260 comprised of the commonly found cyanobacteria *Prochlorococcus* and *Synechococcus* (Silva database
261 classification), as did seawater (mean = $32.26\% \pm 2.46$ SE). Ascidians appeared more variable, with

262 *Rhodobacteraceae*, *Porticoccaceae*, *Cyclobacteriaceae* and unclassified *Alphaproteobacteria*, all abundant
 263 within the top 25 bacteria at the family level.

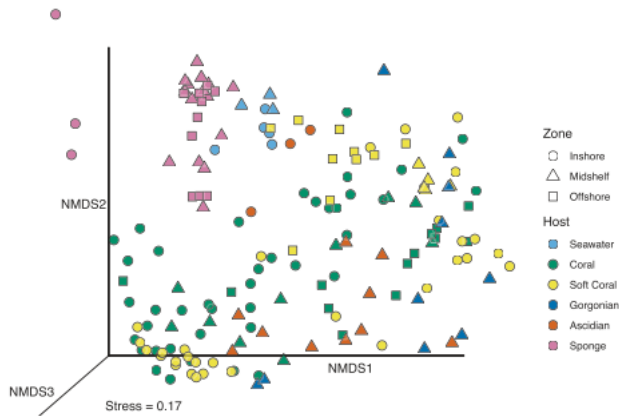


264

265 **Fig. 2** Relative abundance of the top 25 prokaryotic families found across each invertebrate group as well
 266 as seawater and blank extractions. Bubble size is proportional to the relative abundance of each
 267 prokaryotic family (y-axis) within a host group (x-axis).

268

269 Between sample variability (beta diversity) showed there was an overall weak clustering of samples by
 270 their broad taxonomic classifications (Fig. 3). Particularly the three anthozoans (coral, soft coral and
 271 gorgonian) and ascidians had low homogeneity in microbial composition. Comparatively, sponge and
 272 seawater samples formed clusters that indicated consistent microbial composition across samples.
 273 Microbial composition was confirmed statistically to be associated with host taxonomy (PERMANOVA;
 274 $F_{(5, 163)} = 2.58$, $p < 0.001$), however, only a small amount of variation in the data was explained by the
 275 broad taxonomic classification ($R^2 = 0.073$). When samples were instead grouped by host species, the
 276 amount of variation explained increased dramatically (PERMANOVA; $F_{(30, 138)} = 2.01$, $R^2 = 0.30$, $p < 0.001$).
 277 Lastly, beta-diversity analysis showed there was a significant association to collection site (PERMANOVA;
 278 $F_{(6, 162)} = 1.90$, $R^2 = 0.066$, $p < 0.001$), however, only a small amount of variation could be explained by this
 279 variable, and since many species were collected from only one reef, it is likely the variation is due to
 280 species-specific microbiomes.



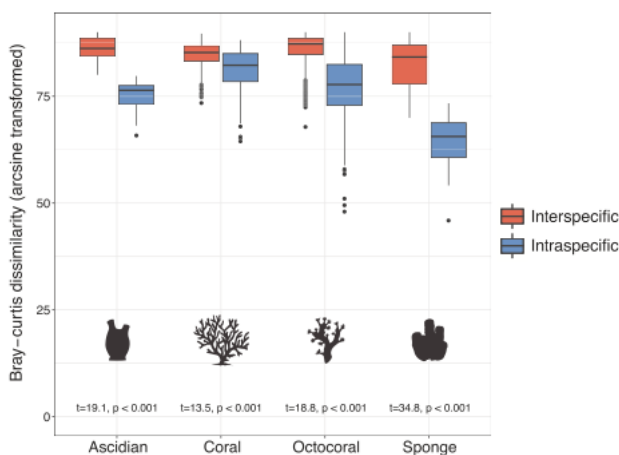
281

282 **Fig. 3** Bray–Curtis dissimilarity based on microbial composition visualised using NMDS. Each symbol
 283 represents a sample where colour is the associated host and shape is reef zone where sample was
 284 collected.

285

286 **Assessment of phyl symbiosis among coral reef invertebrates**

287 All four marine invertebrate groups showed lower intraspecific Bray–Curtis dissimilarity in microbial
 288 composition compared with interspecific Bray–Curtis dissimilarity (coral: $t_{(364)} = 13.53$, $p < 0.001$;
 289 octocoral: $t_{(302)} = 18.84$, $p < 0.001$; sponge: $t_{(200)} = 34.80$, $p < 0.001$; ascidian: $t_{(69)} = 19.09$, $p < 0.001$),
 290 confirming lower microbiome variability among conspecifics (Fig. 4). Furthermore, intraspecific variation
 291 was significantly different among the invertebrate groups (ANOVA; $F_{(3, 818)} = 231.15$, $p < 0.001$), with the
 292 exception of the ascidians and octocorals ($t = 1.85$, $p = 0.39$), highlighting sponges and coral with the
 293 highest and lowest microbiome homogeneity, respectively.



294

295 **Fig. 4** Intraspecific and interspecific Bray–Curtis dissimilarity scores for each invertebrate group.
 296 Interspecific variation (red boxplots) in the microbiome was significantly greater than intraspecific
 297 variation (blue boxplots) for each invertebrate group.

298

299 Comparing the topology of host phylogenetic trees with the corresponding microbial dendrograms (nRF
 300 test) and measuring the correlation of host phylogenetic distance with microbial dissimilarity (Mantel

301 test) further revealed significant levels of phylosymbiosis across all four groups of invertebrates (Table
 302 1). Patterns of phylosymbiosis were significant in sponges using all tests and metrics (Figs. 5a and S4),
 303 while Bray–Curtis and weighted UniFrac metrics found significant patterns of phylosymbiosis using the
 304 nRF and Mantel tests in corals (Figs. 5b and S5a) and octocorals (Figs. 5c and S6a). Using the unweighted
 305 UniFrac distance, phylosymbiosis patterns were significant only using the Mantel test but not the nRF test
 306 for coral (Fig. S5b) and octocoral (Fig. S6b) and no patterns were detected in the ascidians (Fig. S7b).
 307 Perfect congruency between host phylogeny and microbial dendrograms was observed in the ascidians
 308 using both the Bray–Curtis and weighted UniFrac metrics (Figs. 5d and S7a). Despite this, no significant
 309 phylosymbiosis was observed using the Mantel test. This opposing result is likely due to the low sample
 310 size combined with marked differences in microbial composition among the three ascidians (Fig. S8).

311

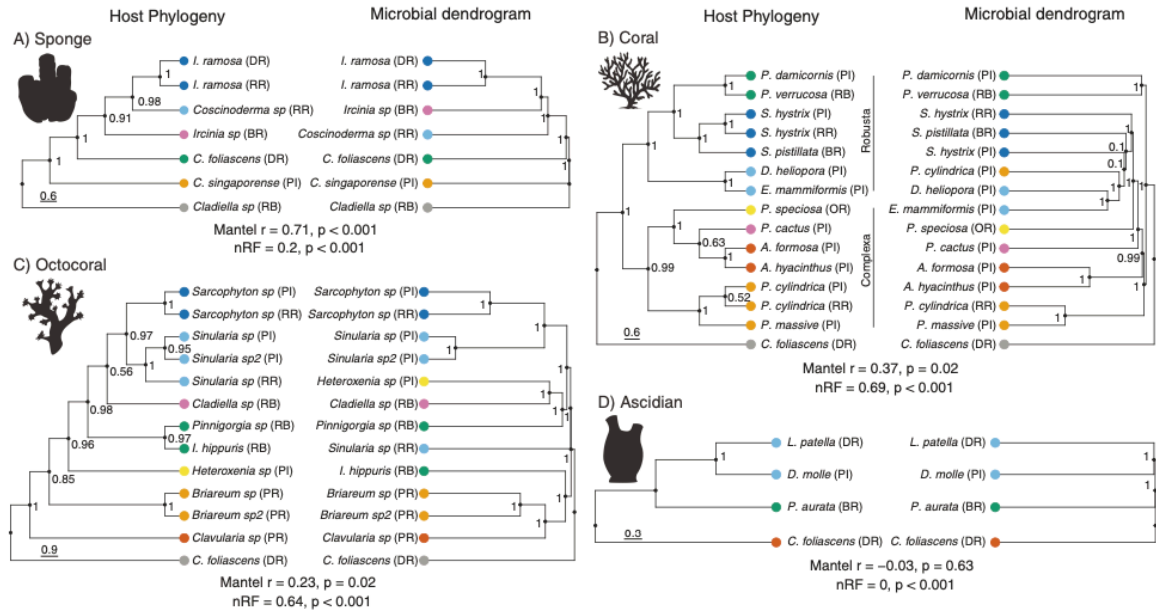
312 **Table 1.** Normalised Robinson–Foulds (nRF) and mantel statistics across Bray–Curtis, weighted and
 313 unweighted UniFrac beta- diversity metrics.

	Bray–Curtis	Weighted UF	Unweighted UF
Sponge			
nRF	RF = 0.02, $p < 0.001$	RF = 0.4, $p = 0.006$	RF = 0.4, $p = 0.01$
Mantel	$r = 0.71$, $p < 0.001$	$r = 0.78$, $p = 0.006$	$r = 0.75$, $p = 0.03$
Coral			
nRF	RF = 0.69, $p < 0.001$	RF = 0.69, $p < 0.001$	RF = 0.92, $p = 0.15$
Mantel	$r = 0.37$, $p = 0.02$	$r = 0.38$, $p = 0.01$	$r = 0.42$, $p = 0.03$
Octocoral			
nRF	RF = 0.64, $p < 0.001$	rRF = 0.82, $p = 0.02$	RF = 0.91, $p = 0.24$
Mantel	$r = 0.23$, $p < 0.001$	$r = 0.36$, $p < 0.001$	$r = 0.25$, $p < 0.001$
Ascidian			
nRF	RF = 0, $p < 0.001$	RF = 0, $p < 0.001$	RF = 0.5, $p = 0.34$
Mantel	$r = -0.03$, $p = 0.63$	$r = 0.46$, $p = 0.17$	$r = 0.18$, $p = 0.46$

314

315

316 A select few species were collected from multiple locations and showed contrasting results in relation to
 317 phylosymbiosis. The sponge *Ircinia ramosa* and octocoral *Sarcophyton* sp. were collected from two
 318 locations and both correctly formed a clade with their conspecifics (Figs. 5, S4 and S6), which was
 319 supported by uniform microbial profiles (Figs. S9 and S10). Conversely, the octocoral *Sinularia* sp. and the
 320 coral species *Porites cylindrica* and *Seriatopora hystrix* did not form clades with their conspecifics from
 321 different locations and there was a reduced overall phylosymbiotic signal (Figs. 5, S5 and S6). A SIMPER
 322 analysis revealed that shifts in the relative abundance of ASVs assigned to *Endozoicomonadaceae* were
 323 consistently the top contributors to the dissimilarity observed between species collected from two sites
 324 (Table S3; Fig. S11). For example, *Porites cylindrica* collected from the Palm Islands (PI) had a dramatic
 325 reduction in *Endozoicomonadaceae* compared with those collected from the RR, where the mean relative
 326 abundance of *Endozoicomonadaceae* fell from 82.9% (± 4.32 SE) to 3.31% (± 1.69 SE). Similarly, the
 327 microbial profile of *Sinularia* collected from RR differed from the two *Sinularia* species collected from PI,
 328 with colonies from RR hosting a lower relative abundance of *Endozoicomonadaceae* and a higher relative
 329 abundance of unknown bacteria and *Fusobacteriaceae* (Fig. S11).



330

331 **Fig. 5** Host phylogeny and microbial dendrogram comparisons for each invertebrate group. a–d Host
 332 phylogenies are inferred from COI, 18S rRNA and ITS1 sequences while microbial dendrograms are based
 333 on Bray–Curtis dissimilarity for microbial composition of each host species. *Cladiella* sp. was used as an
 334 outgroup for a sponges, while *C. foliascens* was used as an outgroup for b coral, c octocoral and d
 335 ascidians. Numbers at nodes reflect posterior probability for clade support in host trees and jackknife
 336 support values in dendrograms. Branch tips are coloured to reflect clades in host phylogeny. Initials in
 337 brackets next to species names refer to collection site. BR Broadhurst Reef, DR Davies Reef, OR Osprey
 338 Reef, PI Palm Islands (Orpheus and Pelorus), PR Pandora Reef, RB Rib Reef, RR Ribbon Reefs. *P. massive*
 339 refers to massive *Porites* sp.

340

341

342 Additional incongruences were observed among the groups where sample location was not a factor. The
 343 overwhelming majority of extant corals fall into one of two major clades, the Robusta and Complexa. This
 344 split was only partially reflected in the Bray–Curtis and weighted UniFrac microbial dendrograms,
 345 although in most cases, species within a genus or family clustered together (Figs. 5b and S5). Similarly,
 346 host phylogeny was recapitulated in the microbiome of only certain clades of octocorals using Bray–
 347 Curtis and weighted UniFrac metrics, such as the microbiome of *Briareum* and species within the family
 348 Alcyoniidae (*Sarcophyton*, *Sinularia* and *Cladiella*), with the exception of *Sinularia* collected from the RR
 349 (Figs. 5c and S6). However, no congruence was seen between gorgonian phylogeny and microbial
 350 composition, which can again be attributed to ASVs assigned to *Endozoicomonadaceae* (Table S3; Fig.
 351 S10). Lastly, although the signal of phyllosymbiosis in sponges was strong and robust across all analyses,
 352 the main incongruence was due to an unclassified *Ircinia* sp., which did not form a clade with its sister
 353 species in the host phylogeny (Fig. 5a), and highlights the unresolved phylogenetic relationships among
 354 the *Ircinia* [51].

355 Discussion

356 This study evaluates the signal of phyllosymbiosis in diverse coral reef invertebrates, finding evidence that
 357 host evolutionary history helps shape the microbiome in sponges, corals, octocorals and ascidians. By
 358 testing three commonly used methods for phyllosymbiosis analysis, we show that all groups have lower
 359 intraspecies microbiome variability compared with interspecies. This was combined with greater
 360 topological congruency between host phylogeny and the microbial dendrogram than would be expected
 361 by chance, except when using the unweighted UniFrac distance in corals, octocorals and ascidians.

362 Interestingly, all invertebrate groups but the ascidians exhibited a significant correlation between host
363 phylogenetic distance and microbial dissimilarity across all beta-diversity metrics.

364 Our results demonstrate that sponges have a strong signature of phylosymbiosis, which likely reflects the
365 uniform microbiome structure in sponges compared with other coral reef invertebrates [18]. This was
366 observed through low intraspecific variation and high homogeneity in the microbiome when the same
367 species was collected from different reefs. Sponges are also known to have a relatively stable microbiome
368 in response to temporal variation and environmental perturbations [52–54]. A stable microbiome may
369 lead to a strong phylosymbiotic signal if there is less influence from the surrounding environment, leaving
370 host factors to be the primary structuring element of the microbiome [53]. Importantly, while sister
371 species were included in the analysis, overall the sponges sampled here span a larger phylogenetic
372 diversity compared with the other groups, which may increase the chance to observe phylosymbiosis. Our
373 results agree with previous conclusions of a significant correlation between host phylogeny and
374 microbiome dissimilarity and validate a prominent role of host phylogeny in shaping the sponge
375 microbiome [18, 55].

376 A signal of phylosymbiosis was demonstrated in coral, which was characterised by a tendency of corals of
377 the same genus or family to cluster together. However, incongruences were observed where the same
378 species was collected from two different locations, primarily due to a shift in the relative abundance of
379 *Endozoicomonadaceae*. Shifts in *Endozoicomonadaceae* have been documented previously, normally in
380 response to host stress [26, 56]. As shifts in the microbial community can often precede visual signs of an
381 unhealthy holobiont [57, 58], it is plausible the decrease in *Endozoicomonadaceae* is linked to an
382 unknown event. Second, coral tissue samples are often contaminated by the coral mucus, which is known
383 to have a dynamic microbial community shifting in composition between new and aged mucus [59].
384 However, bacteria within the tissues of corals are housed within coral-associated microbial aggregates
385 and these communities likely have a more stable association with the host [60, 61]. Therefore, developing
386 approaches to target tissue-specific microbes could be beneficial to understanding phylosymbiosis and
387 other questions related to microbial symbiosis in corals.

388 Similar clustering of coral microbiomes has been observed in Caribbean corals. This partially reflected
389 coral phylogeny, as congeners showed comparatively low microbial dissimilarity and the two major
390 coral clades tended to cluster together, however, inconsistencies were seen when looking at the species
391 level [62], and reflect the results seen here on the GBR. Further evidence of phylosymbiosis in coral was
392 found in an analysis of 691 coral samples collected Australia wide [8]. The endolithic microbial
393 community showed the strongest signal and was the best predictor of the deep phylogeny between the
394 Robusta and Complexa clades. Tissue microbiomes also illustrated evidence of phylosymbiosis, however,
395 the signal was absent in the coral's surface mucus layer. This emphasises an increasing strength of
396 phylosymbiosis where direct environmental factors are reduced. In addition, a small number of microbial
397 lineages, including those within *Endozoicomonadaceae*, demonstrated co-phylogeny with their host, while
398 other clades had a more generalist host distribution. It is possible that host-specialist clades play a minor
399 role in phylosymbiosis through codivergence and future work should aim to untangle the mechanisms
400 behind phylosymbiosis [14].

401 Research on the microbiome structure of octocorals is limited compared with corals, and we show for the
402 first-time direct evidence for phylosymbiosis. The phylosymbiotic signal in octocorals was similar to
403 corals and incongruences also occurred when there was a shift in the relative abundance of
404 *Endozoicomonadaceae*. Octocorals are known to have a more stable and less diverse microbial community
405 than hard corals [63], consistent with our finding that overall microbial diversity was lower and
406 microbiome uniformity higher in octocorals compared with hard corals. While this likely influences the
407 phylosymbiotic signal, a direct comparison between octocorals and corals (and other invertebrate
408 groups) cannot be drawn due to the differences in phylogenetic relatedness between host species.
409 Furthermore, the phylogenetic markers used in this study were chosen to capture both mitochondrial and
410 nuclear evolution across a broad range of diverse species. However, octocorals have poorly understood
411 phylogenetic relationships, with little concordance between morphological, nuclear and mitochondrial
412 data [64]. The incorporation of alternative phylogenetic markers optimised for each taxonomic group
413 may further improve the analyses of phylosymbiosis and comparisons among groups. Finally, octocoral
414 identification in the field is extremely challenging especially when trying to resolve to species level [65].

415 Despite these limitations, we still observe a significant signal of phylosymbiosis, which is likely to
416 strengthen with improved phylogenetic relationships and species identification.

417 Ascidians showed complete congruence between the host phylogeny and microbial dendrogram for both
418 Bray–Curtis and weighted UniFrac metrics, yet no correlation existed between host phylogenetic distance
419 and microbial dissimilarity. Our results therefore do not provide strong support for phylosymbiosis in the
420 group, yet they highlight the need for multiple lines of evidence when evaluating phylo- symbiosis [3]. For
421 example, we find that when sample numbers are low, particularly when marked changes are observed
422 among the microbiomes of host species, the dendrogram approach was more sensitive to patterns of
423 phylosymbiosis compared with the Mantel test. Furthermore, unweighted UniFrac methods were unable
424 to identify a phylosymbiotic signal in the ascidians and had the least power to identify a signal across all
425 invertebrate groups, which agrees with previous conclusions on weighted and unweighted beta-diversity
426 metrics [14]. As this method does not account for the abundance of ASVs, it is less likely to identify beta-
427 diversity patterns in highly diverse microbiomes that are dominated by a relatively small number of
428 bacteria.

429 Our study overwhelmingly found that host phylogeny is reflected in the microbiome of marine
430 invertebrates, particularly notable when considering several confounding factors. Sampling of the reef
431 invertebrates occurred over four field trips that spanned a 1-year timeframe, potentially obscuring
432 phylosymbiosis patterns due to seasonal influences on the microbiome [66]. Furthermore, our samples
433 are from wild colonies collected from multiple locations on the GBR which introduces local environmental
434 differences including water quality and the pelagic communities that serve as host diet. Preservation
435 methods also varied across organisms, including snap freezing and the use of salt saturated dimethyl
436 sulfoxide- EDTA. While these preservation approaches have been shown to have little effect on the
437 microbial composition of coral, it could have influenced alpha diversity [67]. Finally, sample
438 representation differed among the four groups and likely has an important impact on the strength of the
439 phylosymbiosis signal. For example, only three ascidian species (and one outgroup) were used, whereas
440 four related species are recommended [3]. Had more species been included in the analysis, with a larger
441 number of taxonomic sister species, a more reliable representation of phylosymbiosis would likely have
442 been achieved.

443 This is the first study to systematically assess phylosymbiosis among diverse groups of marine
444 invertebrates. We identified a phylosymbiotic signal across all invertebrate groups with multiple
445 methods, of which sponges consistently showed a significant signal using all beta- diversity metrics.
446 Increased intraspecific variability of the microbiome in both scleractinian corals and octocorals was often
447 associated with a change in the relative abundance of *Endozoicomonadaceae*. This microbial family is
448 characterised by host-specialist and host-generalist clades and is assumed to be a dynamic member of the
449 coral holobiont [8]. Host-specialist clades may contribute to phylosymbiosis in corals and octocorals
450 through codivergence, while host- generalist clades obscure the signal through host infidelity. Here, we
451 provide a foundation to begin exploring the mechanisms behind phylosymbiosis and further our
452 understanding on host-microbe symbiosis and coevolution in marine invertebrates.

453 **Data availability**

454 All microbial data have been made available at the NCBI Sequence Read Archive under the BioProject
455 accession number PRJNA577361 and host sequence data are available at the CNGB Sequence Archive
456 under the accession numbers N_000000252.1–N_000000348.1.

457 **Code availability**

458 Code used for the analysis is available at <https://github.com/paobrien>.

459 **Acknowledgements**

460 The authors would like to thank Katharina Fabricius, Georgina Torras and Bettina Glasl for their
461 assistance in the field. We also thank Orpheus Island Research Station and the Molecular Ecology and
462 Evolution Laboratory for facilitating field and laboratory work. We thank Zhenyu Peng, Guohai Hu, Bo

463 Wang, Xudan Li, Wei Zhou, Sha Liao and Junqiang Xu for providing SE400 sequencing. Guohai Hu and Bo
464 Wang are affiliated with Guangdong Provincial Key Laboratory of Genome Read and Write (No.
465 2017B030301011). We also thank Long Zhou and Qiye Li for coordinating the project. This work was
466 funded by the Beijing Genome Institute, Earthwatch Institute and Mitsubishi Corporation. PAO is
467 supported by an AIMS@JCU postgraduate research scholarship.

468 **Author contributions**

469 PAO, DGB, NSW, DJM and GZ conceived and developed the study. PAO, DGB, NSW, PRF and HAS
470 contributed to field work. PAO, ST, CY and HAS contributed to molecular lab work. PAO analysed the
471 microbial data and generated figures and HAS finalised the figures. PAO, ST, CY and NA analysed the
472 phylogenetic data. PAO drafted the paper and all authors revised the paper and approved the final
473 version.

474 **References**

- 475 1. Brooks AW, Kohl KD, Brucker RM, van Opstal EJ, Bordenstein SR. Phylosymbiosis:
476 relationships and functional effects of microbial communities across host evolutionary
477 history. *PLoS Biol.* 2016;14:1–29.
- 478 2. Brucker RM, Bordenstein SR. The hologenomic basis of speciation: gut bacteria cause
479 hybrid lethality in the genus *Nasonia*. *Science.* 2013;341:667–9.
- 480 3. Lim SJ, Bordenstein SR. An introduction to phylosymbiosis. *Proc Biol Sci.*
481 2020;287:20192900.
- 482 4. Brucker RM, Bordenstein SR. The roles of host evolutionary relationships (genus: *Nasonia*)
483 and development in structuring microbial communities. *Evolution.* 2011;66:349–62.
- 484 5. Ochman H, Worobey M, Kuo CH, Ndjango JBN, Peeters M, Hahn BH, et al. Evolutionary
485 relationships of wild hominids recapitulated by gut microbial communities. *PLoS Biol.*
486 2010; 8:3–10.
- 487 6. Kohl KD, Dearing MD, Bordenstein SR. Microbial communities exhibit host species
488 distinguishability and phylosymbiosis along the length of the gastrointestinal tract.
489 *Mol Ecol.* 2018;27:1874–83.
- 490 7. Ross AA, Müller KM, Weese JS, Neufeld JD. Comprehensive skin microbiome analysis
491 reveals the uniqueness of human skin and evidence for phylosymbiosis within the
492 class Mammalia. *Proc Natl Acad Sci.* 2018;115:1–10.
- 493 8. Pollock FJ, McMinds R, Smith S, Bourne DG, Willis BL, Medina M, et al. Coral-associated
494 bacteria demonstrate phylosymbiosis and cophylogeny. *Nat Commun.* 2018;9:1–13.
- 495 9. Yeoh YK, Dennis PG, Paungfoo-Lonhienne C, Weber L, Brackin R, Ragan MA, et al.
496 Evolutionary conservation of a core root microbiome across plant phyla along a
497 tropical soil chronosequence. *Nat Commun.* 2017;8:1–9.
- 498 10. Leigh BA, Bordenstein SR, Brooks AW, Mikaelyan A, Bordenstein SR. Finer-scale
499 phylosymbiosis: insights from insect viromes. *mSystems.* 2018;3:e00131–18.
- 500 11. van Opstal EJ, Bordenstein SR. Phylosymbiosis impacts adaptive traits in *Nasonia* wasps.
501 *MBio.* 2019;10:1–11.
- 502 12. Franzenburg S, Walter J, Künzel S, Wang J, Baines JF, Bosch TCG. Distinct antimicrobial
503 peptide expression determines host species-specific bacterial associations. *Proc Natl*
504 *Acad Sci.* 2013;110:E3730–8.
- 505 13. Douglas AE, Werren JH. Holes in the hologenome: why host- microbe symbioses are not
506 holobionts. *MBio.* 2016;7:e02099–15.

- 507 14. Mazel F, Davis KM, Loudon A, Kwong WK, Groussin M, Parfrey LW. Is host filtering the
508 main driver of phyllosymbiosis across the tree of life? *mSystems*. 2018;3:e00097–18.
509
- 510 15. Groussin M, Mazel F, Sanders JG, Smillie CS, Lavergne S, Thuiller W, et al. Unraveling the
511 processes shaping mammalian gut microbiomes over evolutionary time. *Nat Commun*.
512 2017; 8:1–12.
- 513 16. Hird SM, Sánchez C, Carstens BC, Brumfield RT. Comparative gut microbiota of 59
514 Neotropical bird species. *Front Microbiol*. 2015;6:1–16.
- 515 17. Song SJ, Sanders JG, Delsuc F, Metcalf J, Amato K, Taylor MW, et al. Comparative
516 analyses of vertebrate gut microbiomes reveal convergence between birds and bats.
517 *MBio*. 2020;11:1–14.
- 518 18. Thomas T, Moitinho-Silva L, Lurgi M, Björk JR, Easson C, Astudillo-García C, et al.
519 Diversity, structure and convergent evolution of the global sponge microbiome. *Nat*
520 *Commun*. 2016;7:1–12.
- 521 19. Glasl B, Smith CE, Bourne DG, Webster NS. Disentangling the effect of host-genotype
522 and environment on the microbiome of the coral *Acropora tenuis*. *PeerJ*. 2019;7:1–18.
- 523 20. Amato KR, G. Sanders J, Song SJ, Nute M, Metcalf JL, Thompson LR, et al. Evolutionary
524 trends in host physiology outweigh dietary niche in structuring primate gut
525 microbiomes. *ISME J*. 2019;13:576–87.
- 526 21. Amato KR, Mallott EK, McDonald D, Dominy NJ, Goldberg T, Lambert JE, et al.
527 Convergence of human and Old World monkey gut microbiomes demonstrates the
528 importance of human ecology over phylogeny. *Genome Biol*. 2019;20:1–12.
- 529 22. Sharp KH, Distel D, Paul VJ. Diversity and dynamics of bacterial communities in early life
530 stages of the Caribbean coral *Porites astreoides*. *ISME J*. 2012;6:790–801.
- 531 23. Apprill A, Marlow HQ, Martindale MQ, Rappé MS. The onset of microbial associations in
532 the coral *Pocillopora meandrina*. *ISME J*. 2009;3:685–99.
- 533 24. Webster NS, Taylor MW, Behnam F, Lückner S, Rattei T, Whalan S, et al. Deep sequencing
534 reveals exceptional diversity and modes of transmission for bacterial sponge
535 symbionts. *Environ Microbiol*. 2010;12:2070–82.
- 536 25. O’Brien PA, Webster NS, Miller DJ, Bourne DG. Host-microbe coevolution: applying
537 evidence from model systems to complex marine invertebrate holobionts. *MBio*.
538 2019;10:1–14.
- 539 26. Morrow KM, Bourne DG, Humphrey C, Botté ES, Laffy P, Zaneveld J, et al. Natural
540 volcanic CO₂ seeps reveal future trajectories for host-microbial associations in corals
541 and sponges. *ISME J*. 2014;9:1–15.
- 542 27. Ziegler M, Seneca FO, Yum LK, Palumbi SR, Voolstra CR. Bacterial community dynamics
543 are linked to patterns of coral heat tolerance. *Nat Commun*. 2017;8:1–8.
- 544 28. Parada AE, Needham DM, Fuhrman JA. Every base matters: assessing small subunit rRNA
545 primers for marine microbiomes with mock communities, time series and global field
546 samples. *Environ Microbiol*. 2016;18:1403–14.
- 547 29. Apprill A, McNally S, Parsons R, Weber L. Minor revision to V4 region SSU rRNA 806R
548 gene primer greatly increases detection of SAR11 bacterioplankton. *Aquat Micro Ecol*.
549 2015;75:129–37.
- 550 30. Vrijenhoek R. DNA primers for amplification of mitochondrial cytochrome c oxidase
551 subunit I from diverse metazoan invertebrates. *Mol Mar Biol Biotechnol*. 1994;3:294–
552 9.

- 553 31. Piredda R, Tomasino MP, D'Erchia AM, Manzari C, Pesole G, Montresor M, et al.
554 Diversity and temporal patterns of planktonic protist assemblages at a Mediterranean
555 Long Term Ecological Research site. *FEMS Microbiol Ecol.* 2017;93:fiw200.
- 556 32. Katoh K, Rozewicki J, Yamada KD. MAFFT online service: multiple sequence alignment,
557 interact sequence choice and visualization. *Brief Bioinform.* 2019;20:1160–6.
- 558 33. Yang C, Tan S, Meng G, Bourne DG, O'Brien PA, Xu J, et al. Access COI barcode efficiently
559 using high throughput Single-End 400 bp sequencing. *bioRxiv.* 2018:498618.
- 560 34. Bolyen E, Rideout JR, Dillon MR, Bokulich NA, Abnet CC, AlGhalith GA, et al.
561 Reproducible, interactive, scalable and extensible microbiome data science using
562 QIIME 2. *Nat Biotechnol.* 2019;37:852–7.
- 563 35. Callahan BJ, McMurdie PJ, Rosen MJ, Han AW, Johnson AJA, Holmes SP. DADA2: High-
564 resolution sample inference from Illumina amplicon data. *Nat Methods.* 2016;13:581–
565 3.
- 566 36. Janssen S, McDonald D, Gonzalez A, Navas-Molina JA, Jiang L, Xu ZZ, et al. Phylogenetic
567 placement of exact amplicon sequences improves associations with clinical
568 information. *mSystems.* 2018;3:1–14.
- 569 37. Team RC. R: A language and environment for statistical computing. Vienna: R Foundation
570 for Statistical Computing; 2018. <https://www.r-project.org/>.
- 571 38. McMurdie PJ, Holmes S. Phyloseq: an R package for reproducible interactive analysis and
572 graphics of microbiome census data. *PLoS One.* 2013;8:1–11.
- 573 39. Oksanen J, Blanchet G, Friendly M, Kindt R, Legendre P, McGlinn D, et al. vegan:
574 community ecology package. R package version. 2019;2:5–4.
- 575 40. Wickham H. ggplot2: elegant graphics for data analysis. New York: Springer-Verlag;
576 2016. <http://ggplot2.org>.
- 577 41. Yu G, Smith D, Zhu H, Guan Y, Tsan-Yuk Lam T. ggtree: an R package for visualization and
578 annotation of phylogenetic trees with their covariates and other associated data.
579 *Methods Ecol Evol.* 2017;8:28–36.
- 580 42. Paradis E, Schliep K. ape 5.0: an environment for modern phylogenetics and evolutionary
581 analyses in R. *Bioinformatics.* 2018; 35:526–8.
- 582 43. Schliep K. phangorn: phylogenetic analysis in R. *Bioinformatics.* 2011;27:592–3.
- 583 44. Wickham H, François R, Henry L, Müller K. dplyr: a grammar of data manipulation. R
584 package version 0.8.0.1. 2019. <https://CRAN.R-project.org/package=dplyr>.
- 585 45. McKnight DT, Huerlimann R, Bower DS, Schwarzkopf L, Alford RA, Zenger KR. Methods
586 for normalizing microbiome data: an ecological perspective. *Methods Ecol Evol.*
587 2019;10:389–400.
- 588 46. Edgar RC. MUSCLE: multiple sequence alignment with high accuracy and high
589 throughput. *Nucleic Acids Res.* 2004;32: 1792–7.
- 590 47. Xia X, Xie Z. DAMBE: software package for data analysis in molecular biology and
591 evolution. *J Hered.* 2001;92:371–3.
- 592 48. Castresana J. Selection of conserved blocks from multiple alignments for their use in
593 phylogenetic analysis. *Mol Biol Evol.* 2000;17:540–52.
- 594 49. Darriba D, Taboada GL, Doallo R, Posada D. jModelTest 2: more models, new heuristics
595 and parallel computing. *Nat Methods.* 2012;9:772.
- 596 50. Ronquist F, Teslenko M, Van Der Mark P, Ayres DL, Darling A, Höhna S, et al. MrBayes
597 3.2: efficient Bayesian phylogenetic inference and model choice across a large model
598 space. *Syst Biol.* 2012;61:539–42.

- 599 51. Pöppe J, Sutcliffe P, Hooper JNA, Wörheide G, Erpenbeck D. CO I barcoding reveals new
600 clades and radiation patterns of indo- pacific sponges of the family irciniidae
601 (Demospongiae: Dictyoceratida). PLoS One. 2010;5:1–6.
- 602 52. Erwin PM, Coma R, Paula L, Serrano E, Ribes M, Mar P. Stable symbionts across the
603 HMA-LMA dichotomy: low seasonal and interannual variation in sponge-associated
604 bacteria from taxonomically. FEMS Microbiol Ecol. 2015;91:1–11.
- 605 53. Glasl B, Smith CE, Bourne DG, Webster NS. Exploring the diversity-stability paradigm
606 using sponge microbial communities. Sci Rep. 2018;8:1–9.
- 607 54. Luter HM, Whalan S, Webster NS. Thermal and sedimentation stress are unlikely causes
608 of brown spot syndrome in the coral reef sponge, *Ianthella basta*. PLoS One.
609 2012;7:e39779.
- 610 55. Easson CG, Thacker RW. Phylogenetic signal in the community structure of host-specific
611 microbiomes of tropical marine sponges. Front Microbiol. 2014;5:1–11.
- 612 56. Meyer JL, Paul VJ, Teplitski M. Community shifts in the surface microbiomes of the coral
613 *Porites astreoides* with unusual lesions. PLoS One. 2014;9:e100316.
- 614 57. Bourne D, Iida Y, Uthicke S, Smith-keune C. Changes in coral- associated microbial
615 communities during a bleaching event. ISME J. 2008;2:350–63.
- 616 58. Pollock FJ, Lamb JB, Water JAJM Van De, Smith HA, Schaffelke B, Willis BL. et al. Reduced
617 diversity and stability of coral-associated bacterial communities and suppressed
618 immune function precedes disease onset in corals. R Soc Open Sci. 2019;6:190355
- 619 59. Glasl B, Herndl GJ, Frade PR. The microbiome of coral surface mucus has a key role in
620 mediating holobiont health and survival upon disturbance. ISME J. 2016;10:2280–92.
- 621 60. Work TM, Aeby GS. Microbial aggregates within tissues infect a diversity of corals
622 throughout the Indo-Pacific. Mar Ecol Prog Ser. 2014;500:1–9.
- 623 61. Wada N, Ishimochi M, Matsui T, Pollock FJ, Tang S, Ainsworth TD, et al. Characterization
624 of coral-associated microbial aggregates (CAMAs) within tissues of the coral *Acropora*
625 *hyacinthus*. Sci Rep. 2019;9:1–13.
- 626 62. Sunagawa S, Woodley CM, Medina M. Threatened corals provide underexplored
627 microbial habitats. PLoS One. 2010;5:1–7.
- 628 63. Van De Water JAJM, Allemand D, Ferrier-Pagès C. Host-microbe interactions in octocoral
629 holobionts—recent advances and perspectives. Microbiome. 2018;6:1–28.
- 630 64. McFadden CS, Sánchez JA, France SC. Molecular phylogenetic insights into the evolution
631 of octocorallia: a review. Integr Comp Biol. 2010;50:389–410.
- 632 65. Quattrini AM, Wu T, Soong K, Jeng M, Benayahu Y, Mcfadden CS. A next generation
633 approach to species delimitation reveals the role of hybridization in a cryptic species
634 complex of corals. BMC Evol Biol. 2019;19:1–19.
- 635 66. Li J, Chen Q, Long LJ, Dong JD, Yang J, Zhang S. Bacterial dynamics within the mucus,
636 tissue and skeleton of the coral *Porites lutea* during different seasons. Sci Rep. 2014;4:
637 1–8.
- 638 67. Hernandez-Agreda A, Leggat W, Ainsworth TD, Hernandez- Agreda A. A comparative
639 analysis of microbial DNA preparation methods for use with massive and branching
640 coral growth forms. Front Microbiol. 2018;9:1–14.
- 641